Journal of Magnetism and Magnetic Materials 505 (2020) 166730

Contents lists available at ScienceDirect

Journal of Magnetism and Magnetic Materials

journal homepage: www.elsevier.com/locate/jmmm

Research articles

Rabi-like quantum communication in an aperiodic spin-1/2 chain

D. Messias, C.V.C. Mendes, G.M.A. Almeida, M.L. Lyra, F.A.B.F. de Moura*

Instituto de Física, Universidade Federal de Alagoas, Maceió, AL 57072-970, Brazil

ARTICLE INFO

Keywords:
Aperiodic Sarma potential
Entanglement
Extended states

ABSTRACT

We study a quantum-state transfer protocol across a 1D *XY* spin-1/2 channel featuring on-site magnetic field distribution following the aperiodic Sarma potential. The scheme is based upon weakly connecting the sender and receiver to the channel at each end. Our results show that such aperiodicity allows for high-fidelity performance as a band of extended states near the band center is created and the outer parts of the system are properly tuned with it. We also evaluate the generation of bipartite entanglement shared among the communicating parties.

1. Introduction

Transmitting quantum states (e.g. a qubit) and generating entanglement at arbitrary distances are essential tasks in quantum networks and distributed quantum information processing [1,2]. In this context, the idea of pre-engineered quantum spin chains as put forward by Bose in [3] is based on having minimal control over the system during realization of the protocol so as to avoid decoherence and other forms of noise. The ke point is to set the network, its coupling patterns, and local magnetic fields in advance, and then let it evolve following its own Hamiltonian dynamics (for reviews, cf. [4,5]). Proper initialization of the system and precise knowledge over the dynamics timescale are also necessary and that is where one of the major drawbacks comes about.

Static (e.g. fabrication errors) and/or dynamic fluctuations of the system parameters may compromise our ability to predict when and where the quantum state will be at a certain location [6]. Disorder, for instance, may promote Anderson localization thereby affecting the performance of the communication protocol [7,8]. While this happens to be true for one- and twodimensional models with on-site *uncorrelated* disorder (for any disorder strength), correlated fluctuations can break this rule for they are capable of sustaining extended states in some parts of the spectrum [9]. For instance, it was shown long time ago that long-range-correlated disorder induces a metal–insulator transition with sharp mobility edges [10,11]. This was confirmed by experiments performed on waveguides [12,13]. Quite recently, a single-particle mobility edge has also been reported [14] on a 1D quasiperiodic optical lattice thereby setting the ground for further, more demanding physical implementations.

Overall, although most of the coupling schemes for quantum-state transfer (QST) protocols may hold against small amounts of disorder [15–23], a particular one has been shown to be relatively robust against it. Weak-coupling models [24,25] happen to hide those imperfections away as the sender and receiver are perturbatively connected to the channel. The communicating parties effectively get in touch via the few channel modes they are mostly tuned with. One particular scenario is the generation of a reduced two-level (or Rabi-like) dynamics, up to second-order perturbation theory, between the sender and receiver with renormalized coupling and on-site energies [25]. Such a class of systems has also been addressed in the context of, e.g., entanglement generation [15,26,27] and routing protocols [28].

Recent works have shown that various types of correlated disorder allows for performance of Rabi-like QST with high fidelities [6,29]. One of the crucial requirements for the channel is that it features a band of extended states so as to induce an effective two-level resonance within the perturbation framework [30]. Therefore, the search for models displaying coexistence between localized and delocalized states is paramount. In this work we are to unveil the capability of a *XY* spin channel featuring an on-site magnetic field distribution following the aperiodic slowly varying series introduced by Das Sarma et al. in [31,32]. This is a special class of deterministic one-dimensional potentials that exhibit mobility edges separating localized and extended states. Several works have been devoted to study the electronic transport properties in such aperiodic potential [33–43], including the onset of Bloch oscillations under the action of a uniform external field [35], topological states, and phase transitions [42,43]. Further, quantum information measures have been shown to be able to capture the localization-delocalization transition in these systems [36–39]. However, the actual capability of entanglement generation and QST protocols through channels with engineered slowly varying aperiodic modulation

* Corresponding author.
E-mail address: fidelis@fis.ufal.br (F.A.B.F. de Moura).

https://doi.org/10.1016/j.jmmm.2020.166730
Received 5 November 2019; Received in revised form 28 February 2020; Accepted 9 March 2020
Available online 12 March 2020

of an external field are still open issues.

Considering the above, here we investigate the performance of the standard QST scheme [3] as well as of end-to-end entanglement generation in the weak-coupling model [24,25]. We find that the channel aperiodicity allows for high-quality performances for a wide range of parameters, with a speed-fidelity tradeoff comparable to the uniform case which is known to be optimal [30]. We relate such figure of merit with the known localization-delocalization properties of the model. Moreover, due to the finiteness of the channel, we report a regime where even though localization would set about in the thermodynamic limit, QST still succeeds with good fidelity.

2. Hamiltonian model

The system we consider here is a 1D isotropic spin− 1/2 chain featuring exchange interactions of the XY-type among its $N + 2$ spins, as described by the Hamiltonian ($\hbar = 1$)

$$\widehat{H} = \sum_{i=1}^{N+2} \frac{\epsilon_i}{2}\left(\hat{1} - \hat{\sigma}_i^z\right) + \sum_{i=1}^{N+1} \frac{J_i}{2}\left(\hat{\sigma}_i^x\hat{\sigma}_{i+1}^x + \hat{\sigma}_i^y\hat{\sigma}_{i+1}^y\right), \tag{1}$$

where $\hat{\sigma}_i^{x,y,z}$ are the Pauli spin operators for a spin residing at the i-th site, ϵ_i is the local magnetic field strength, and J_i is the spin exchange coupling strength, henceforth taken to be $J_1 = J_{N+1} = g$ and $J_i = J \equiv 1$ else, with $g \ll J$. That is to say the outer spins are weakly connected to a spin channel with uniform couplings. We also set $\epsilon_1 = \epsilon_{N+2} = W$.

The protocol goes as follows [3]. Suppose the first spin (sender) is prepared in an arbitrary state $|\phi\rangle_1 = a|0\rangle_1 + b|1\rangle_1$ — with $|0\rangle$ ($|1\rangle$) denoting spin down (up) — with the remaining ones in the ferromagnetic ground state, what makes the initial state of the whole system $|\Psi(0)\rangle = |\phi\rangle_1|\mathbf{0}\rangle_{\text{channel}}|0\rangle_{N+2}$, where $|\mathbf{0}\rangle_{\text{channel}} = |0\rangle_2\cdots|0\rangle_{N+1}$. We then let it evolve through its natural Hamiltonian dynamics so that at time t we have $|\Psi(t)\rangle = e^{-iHt}|\Psi(0)\rangle$. It is immediate to see that only the ket featuring a single excitation (spin up) will actually contribute to propagation along the chain as the isotropic XY (or just XX) Hamiltonian preserves the number of excitations. Thus the dynamics is restricted to the subspace spanned by $|i\rangle = |0\rangle_1|0\rangle_2\cdots|1\rangle_i\cdots|0\rangle_{N+2}$, denoting a single spin flipped at the i-th site.

At some specific time τ, the ultimate goal is to find $|\Psi(\tau)\rangle = |0\rangle_1|\mathbf{0}\rangle_{\text{channel}}|\phi\rangle_{N+2}$ (up to a global phase) in order to get the fidelity $F_\phi = \langle\phi|\rho_{N+2}|\phi\rangle$ as high as possible, with $\rho_{N+2} = \text{Tr}_{1,\ldots,N+1}|\Psi(\tau)\rangle\langle\Psi(\tau)|$. A proper function to measure the performance of the protocol can be obtained from averaging over every possible input combination (a, b), that is over the Bloch sphere. It results in the so-called averaged fidelity [3]

$$F(t) = \frac{1}{2} + \frac{f_{N+2}(t)}{3}\cos\vartheta + \frac{f_{N+2}(t)^2}{6}, \tag{2}$$

where $f_j(t) = |\langle j|e^{-iHt}|1\rangle|$is the absolute value of the transition amplitude and its associated phase ϑ can generally be ignored by a convenient choice of the local magnetic fields (we set $\cos\vartheta = 1$ hereafter). Note that outcomes of Eq. (2) are within [0.5, 1], only being maximum when $f_{N+2}(t) = 1$.

At this point it is better to rewrite the system Hamiltonian as

$$\begin{aligned} H = {} & H_{\text{channel}} + W(|1\rangle\langle 1| + |N+2\rangle\langle N+2|) \\ & + g(|1\rangle\langle 2| + |N+1\rangle\langle N+2|) + \text{H. c.}, \end{aligned} \tag{3}$$

on basis $\{|i\rangle\}$, with $H_{\text{channel}} = \sum_{j=2}^{N+1}\epsilon_j|j\rangle\langle j| + J\sum_{j=2}^{N}|j\rangle\langle j+1| + \text{H. c.}$. By coupling the outer (communicating) spins very weakly ($g \ll J$) to the channel we expect them to be energetically detached from the rest of the chain thereby generating their own subspace and behaving like an effective two-level system. As a matter of fact, using second-order perturbation theory in g, we can obtain [25]

$$H_{\text{eff}} = \begin{pmatrix} h_L & J_{\text{eff}} \\ J_{\text{eff}} & h_R \end{pmatrix}, \tag{4}$$

with

$$h_\nu = W - g^2\sum_k \frac{|a_{\nu,k}|^2}{\lambda_k - W}, \tag{5}$$

$$J_{\text{eff}} = -g^2\sum_k \left(\frac{a_{L,k}a_{R,k}^*}{\lambda_k - W}\right), \tag{6}$$

where $\nu \in \{L, R\}$, $a_{L,k} \equiv \langle 2|\lambda_k\rangle$, $a_{R,k} \equiv \langle N+1|\lambda_k\rangle$, with $|\lambda_k\rangle$ and λ_k being, respectively, the eigenstates and eigenvalues of H_{channel}.

Once the conditions for generating the above effective two-level system are set — that is $W \neq \lambda_k\ \forall\ k$ and $g \ll J$ — we still need to be sure whether or not it allows for full, resonant end-to-end Rabi oscillations. Straightforward diagonalization of Hamiltonian (4) yields

$$f_{N+2}^{(\text{eff})}(t) = \frac{2|J_{\text{eff}}|}{\Omega}\left|\sin\left(\frac{\Omega t}{2}\right)\right|, \tag{7}$$

where $\Omega = \sqrt{\Delta^2 + 4J_{\text{eff}}^2}$, with $\Delta = h_L - h_R$. The transition amplitude then reaches its maximum at times $t = \tau = n\pi/\Omega$ for odd n and yields to unit fidelity only when $\Delta = 0$, leading to $\tau = n\pi/2|J_{\text{eff}}|$. Note that the transfer time τ is $O(g^{-2})$. It is also relevant to highlight that at half of the QST time, one can obtain a Bell-type entangled state [24]:

$$\begin{aligned} & |1\rangle_1|0\rangle_{N+2}|\mathbf{0}\rangle_{\text{channel}} \\ & \rightarrow \tfrac{1}{\sqrt{2}}(|1\rangle_1|0\rangle_{N+2} - |0\rangle_1|1\rangle_{N+2})|\mathbf{0}\rangle_{\text{channel}}. \end{aligned} \tag{8}$$

For this reason, here we are also interested in evaluating the concurrence [44] between the sender and receiver spins which, in the computational basis, is expressed as

$$C(t) = 2f_1(t)f_{N+2}(t), \tag{9}$$

which goes from 0 (no entanglement) to 1 (maximum entanglement). Using the expressions obtained via perturbation theory, we get

$$C(t) = \frac{4|J_{\text{eff}}|}{\Omega^2}\sqrt{\Delta^2 + 4J_{\text{eff}}^2\cos^2\left(\frac{\Omega t}{2}\right)}\left|\sin\left(\frac{\Omega t}{2}\right)\right|. \tag{10}$$

If $\Delta = 0$ then $C(t) = |\sin(\Omega t)|$ and maximum entanglement can be recorded at times $t = n\tau/2 (n = 1, 3, \ldots)$, as expected.

In the case of asymmetries within the channel, such as in the presence of an aperiodic magnetic-field distribution, one should expect $\Delta \neq 0$. In other words, these fluctuations become single-site defects in the effective two-level description [Eq. (4)]. Still, the protocol is bound to work if we somehow guarantee $|\Delta| \ll |J_{\text{eff}}|$ at least. It has been shown that such condition holds even in the presence of disorder as long as it is of special kinds [6].

Here, we set the local magnetic fields within the channel to follow an aperiodic series of the form [31,32]

$$\epsilon_j = V\cos(2\pi\alpha j^\nu), \tag{11}$$

($j = 2, 3, \ldots, N+1$) where $V > 0$, $\nu > 0$, and α ultimately set the localization properties of the system. If α is rational and ν an integer, one gets a periodic Bloch potential. For an irrational value of α with $\nu = 1$, Harper's equation is obtained whereas for $\nu \geqslant 2$ it becomes statistically equivalent to the random Anderson model. Keeping α irrational, for $0 < \nu < 1$ and $V < 2J$, there is a phase of extended states near the band center, bounded by two mobility edges located at $E_c = \pm(2J - V)$, separating them from localized states. All states are found to be localized whenever $V > 2J$ or $1 < \nu < 2$, although the Lyapunov exponent approaches zero slowly at the band center for the latter [31,32].

3. Results

Those ubiquitous channel properties allow us to perform high-fidelity QST as long as we tune the frequency of the outer spins, W, to the band center to make use of the available extended states. An inspection in Eqs. (5) and (6) tells us that, if $a_{L,k}$ and $a_{R,k}$ are well distributed throughout the spectrum — mostly in the vicinity of W given each term

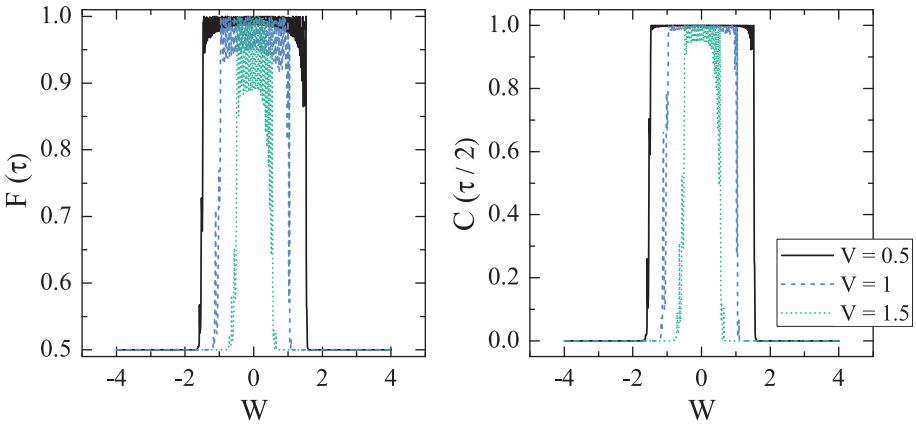

Fig. 1. Averaged fidelity $F(\tau)$ and concurrence $C(\tau/2)$, evaluated for $\tau = \pi/\Omega$, obtained via second-order perturbation theory. We set $N = 100$, $\nu = 0.5$, $\pi\alpha = 0.5$, and $V/J = 0.5$, 1, 1.5. Plots indicate that channel modes within $[-2J + V, 2J - V]$ indeed feature an extended character (given $\nu < 1$).

in the sum $\sim(\lambda_k - W)^{-1}$ — meaning that the sum runs over extended states, it is very likely that $|\Delta| \ll |J_{\text{eff}}|$, yielding $F(\tau) \approx 1$ and $C(\tau/2) \approx 1$.

To see that, in Fig. 1 we plot the fidelity and concurrence against W using the results obtained via perturbation theory, Eqs. (7) and (10). In order to properly compare those to exact diagonalization of the full Hamiltonian [Eq. (1)] and as we set a diverse parameter configurations throughout our analysis, we choose to track the maximum fidelity $F_{\max}$ and maximum concurrence $C_{\max}$ recorded over a wide time window. For now, that will do the job in telling us whether or not the aperiodic channel we consider fulfills the requirements for performing Rabi-like communication protocols. Results are displayed in Figs. 2 and 3 for various α values and fixed $V = 1J$. We readily see that it goes as predicted by perturbation theory (Fig. 1) for small enough g for it ultimately prevents the excitation to populate the channel during realization of the protocol. Note that larger channels demands smaller g as more modes spanned around W may cause further mixing with the sender/receiver subspace. A significant performance loss is seen in Figs. 2 and 3 for $g = 0.1J$ upon going from $N = 50$ to $N = 100$. Another detail is that, overall, α does not bring any significant difference as long as it is kept irrational.

Those figures embody our most representative results for the QST and entanglement generation protocols. They reveal that when W is set around the center of the band, faithful quantum communication between spins 1 and $N + 2$ is made possible, as told out by the nearly unit QST fidelity and the high degree of bipartite entanglement shared between the ends of the chain. This is valid for $W \in [-2J + V, 2J - V]$

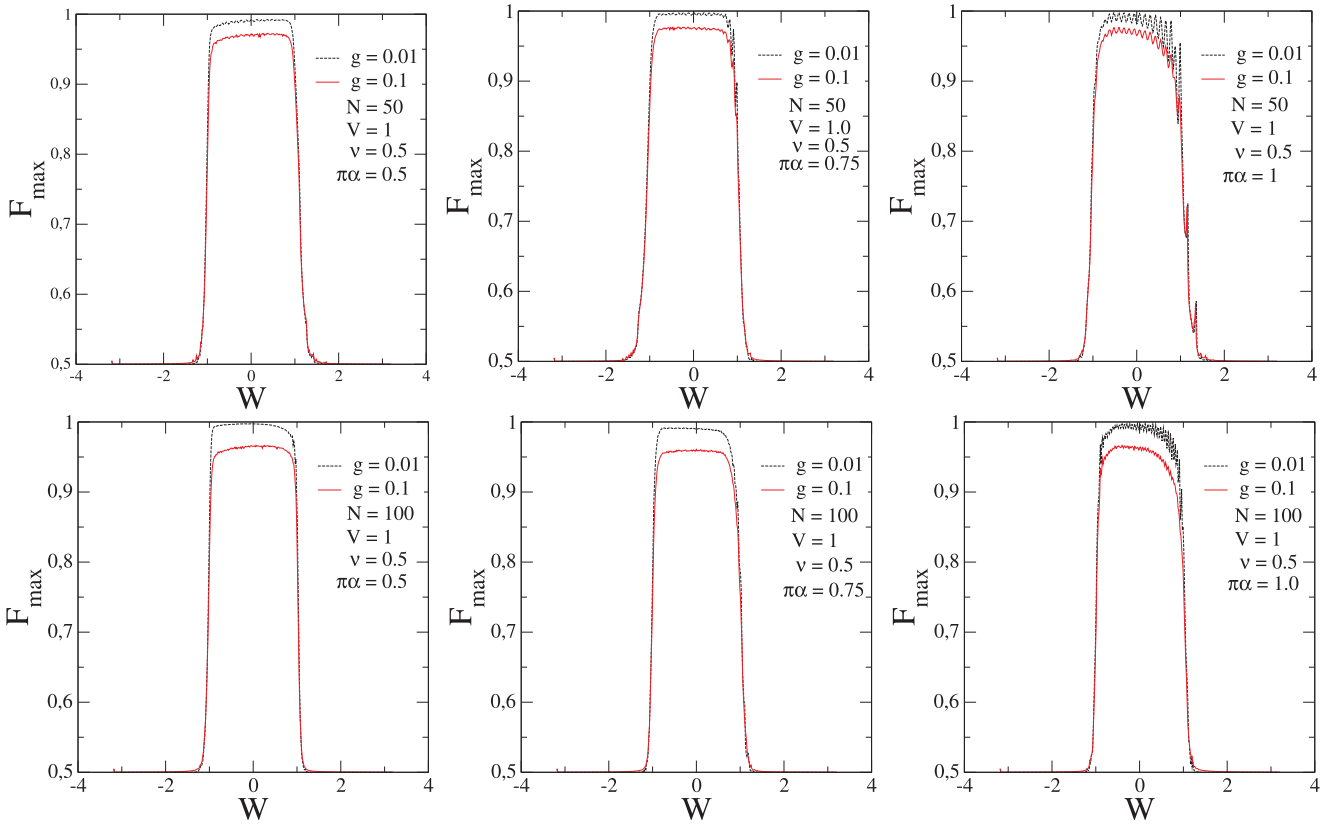

Fig. 2. Maximum fidelity $F_{\max} = \max\{F(t)\}$ over $tJ \in [0, 10^5]$ versus W for $N = 50$, 100, $g/J = 0.1$, 0.01, $V/J = 1$, $\nu = 0.5$, and $\pi\alpha = 0.5$, 0.75, 1 obtained from exact numerical diagonalization of the full Hamiltonian, Eq. (1). Plots show that high-fidelity QST occurs within the band of extended states as predicted for the aperiodic channel, i.e, within $[-2J + V, 2J - V]$.

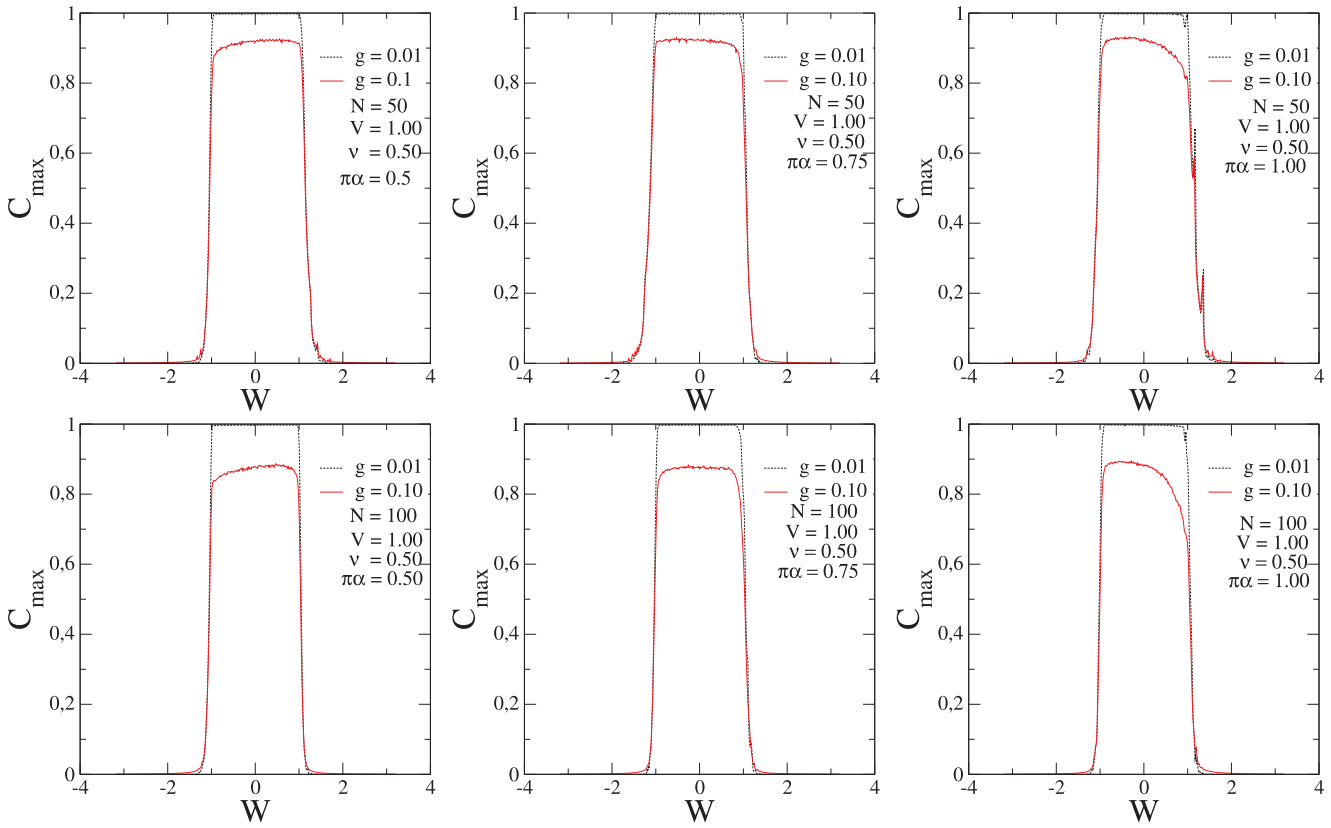

Fig. 3. Maximum concurrence $C_{\max} = \max\{C(t)\}$ over $tJ \in [0, 10^5]$ versus W for $N = 50, 100$, $g/J = 0.1, 0.01$, $V/J = 1$, $\nu = 0.5$, and $\pi\alpha = 0.5, 0.75, 1$ obtained from exact numerical diagonalization of the full Hamiltonian, Eq. (1). For $-1J < W < 1J$ the sender (spin 1) and receiver (spin $N + 2$) share nearly-maximum entanglement thereby corroborating with the results seen in Fig. 2.

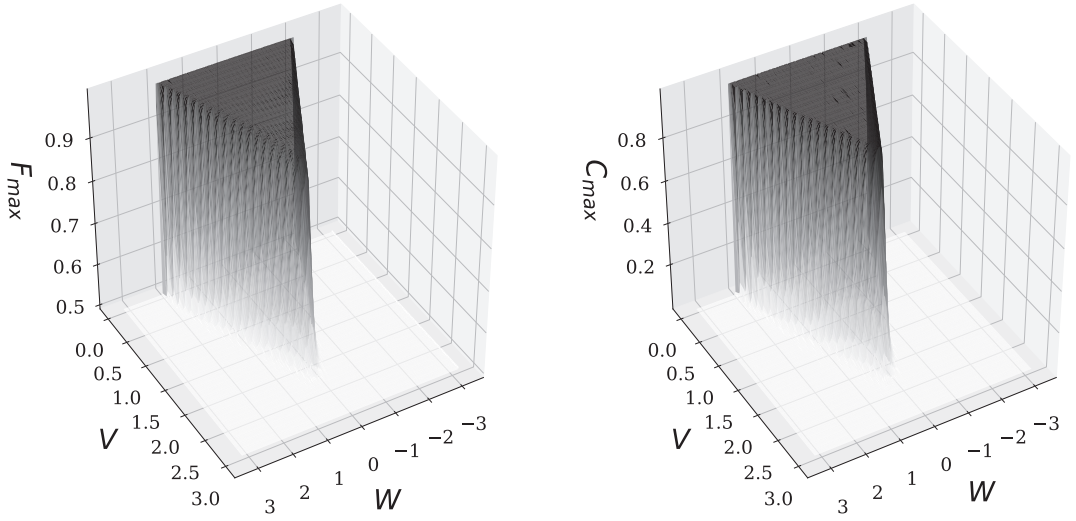

Fig. 4. $F_{\max}$ and $C_{\max}$ over $tJ \in [0, 10^5]$ versus W and V for $N = 100$, $\nu = 0.5$, $g = 0.01J$, and $\pi\alpha = 0.5$, obtained via exact numerical diagonalization of Hamiltonian (1).

which is the energy range contaning delocalized states for $\nu < 1$ [31,32]. Fig. 1 indeed shows that the width of the region in which best-quality performances are obtained gets narrower upon increasing V. To provide with another point of view, in Fig. 4 we evaluate both figures of merit versus W and V for $\nu = 0.5$ and $g = 0.01J$ via full exact numerical diagonalization and confirm that such width decreases linearly.

Now, we fix both $F_{\max}$ and $C_{\max}$ to $W = 0$ and focus on the role of V and ν [cf. Eq. (11)] on the performances in Fig. 5, therein also comparing results obtained via perturbation theory and exact numerical diagonalization of the full spin Hamiltonian. We spot a interesting behavior surrounding $V \approx 2J$ above which QST and entanglement generation begin to fade [see Fig. 5(a) and (c)]. This is again in agreement with the localization properties of the apperiodic potential as for $V > 2J$ all eigenstates within the channel are localized [31,32]. In Fig. 5(b) and (d) we see that $\nu \gg 1$ rules out the possibility of carrying out faithful quantum communication, a expected feature since $\nu > 1$ yields localization throughout the whole spectrum [31,32].

Curiously though, for ν slightly greater than 1 we can still observe relatively good performances. We emphasize that the critical point $\nu = 1$ for the localization-delocalization transition in apperiodic models was obtained in several works using distinct methods (see e.g. Refs. [31,32,45,46]) and it is known that the localization length around the

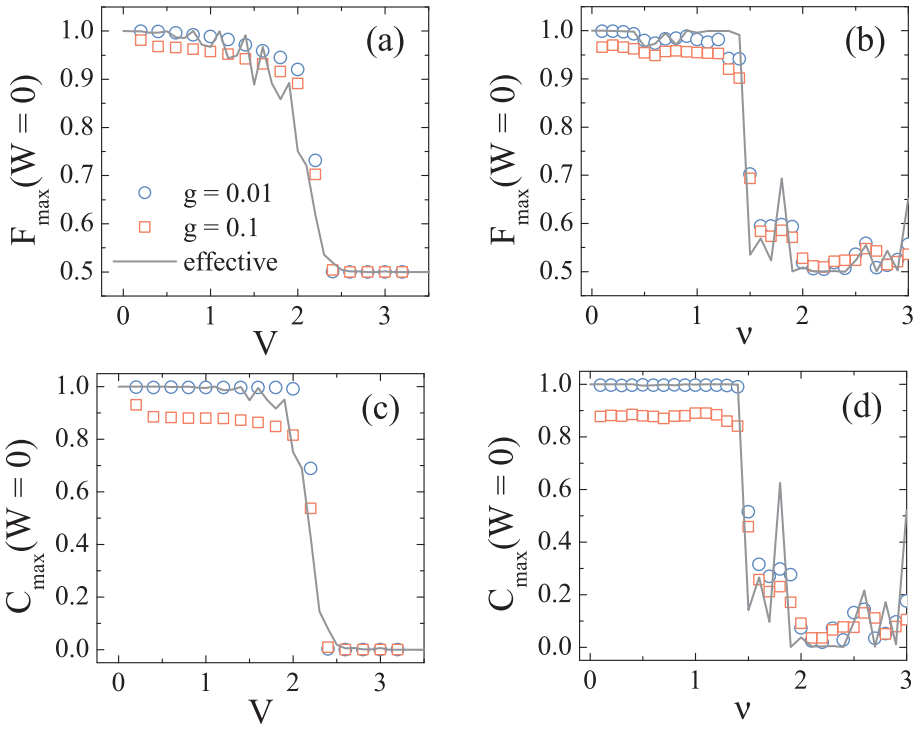

Fig. 5. Maximum fidelity $F_{\max}$ and concurrence $C_{\max}$ for fixed $W = 0$ (a,c) versus V for fixed $\nu = 0.5$ and (b,d) versus ν for $V = 1J$. In all plots, $N = 100$ and $\pi\alpha = 0.1$ and we display results obtained from exact numerical diagonalization of the full Hamiltonian, [Eq. (1)] for $g = 0.01J$ (blue circles) and $g = 0.1J$ (red squares), recorded over $tJ \in [0, 10^5]$, alongside the effective description via second-order perturbation theory (solid gray lines), that is $F_{\max} \equiv F(\tau)$ and $C_{\max} \equiv C(\tau/2)$, with $\tau = \pi/\Omega$, as evaluated from Eqs. (7) and (10).

band center ($W = 0$) is large, covering about 10^3–10^4 sites. Therefore, for $\nu \approx 1$ and given that we are dealing with small channels ($N = 10^2$) the localization length is in general larger that N, what promotes relatively good outcomes for $F_{\max}$ and $C_{\max}$.

So far we have been investigating the performance of the protocols in a broad time window. In practice, though, one must know in advance how long it takes, with reasonable precision, to transmit a quantum state from one point to another or when entanglement will be established between two nodes of a quantum network in order to carry on with the computation (either measuring the state or routing it to somewhere else).

A major issue with weak-coupling models is that the transfer time scales as $\tau \sim g^{-2}$ and so, as the very onset of Rabi-like dynamics requires g to be rather small, one should expect long times to get a nearly unit fidelity. It was proved in Ref. [30] that channels with uniform coupling strengths provide with the optimal speed-fidelity tradeoff given the on-site energies are also on the same level ($\epsilon_i = \epsilon$). This means that the homogeneous channel outperforms in terms of fidelity when comparing with any other coupling scheme, both operating with the same QST time. The homogeneous channel features $\Delta = 0$, $J_{\text{eff}} = -g^2/J$ and then $\tau = \pi J/2g^2$ while the fidelity of the transfer scales as $F = 1 - O(g^2 N)$, what demands $g \ll 1/\sqrt{N}$ [24]. In general, one may reduce the transfer time with cost of compromising fidelity.

We now use the homogeneous channel as a reference and see about the speed-fidelity tradeoff against the aperiodic channel for various parameters. Let us first define $\widetilde{\Omega} = \Omega J/g^2$, rendering $\tau = \pi J/g^2\widetilde{\Omega}$. Setting $g = \delta J/\sqrt{\widetilde{\Omega}}$ for every channel, the expected transfer time becomes $\tau = \pi/J\delta^2$. Having placed a configuration-independent τ, we are now in position to evaluate the corresponding fidelities. Results are shown in Fig. 6 and we readily see that, despite the asymmetry of the channel, the aperiodic sequence of magnetic fields throughout the chain holds a performance comparable to that of the homogeneous channel ($V = 0$; solid lines), albeit for some values of ν and especially for higher V, for it is seen that the fidelity saturates to values <1 even as $\delta \to 0$, meaning

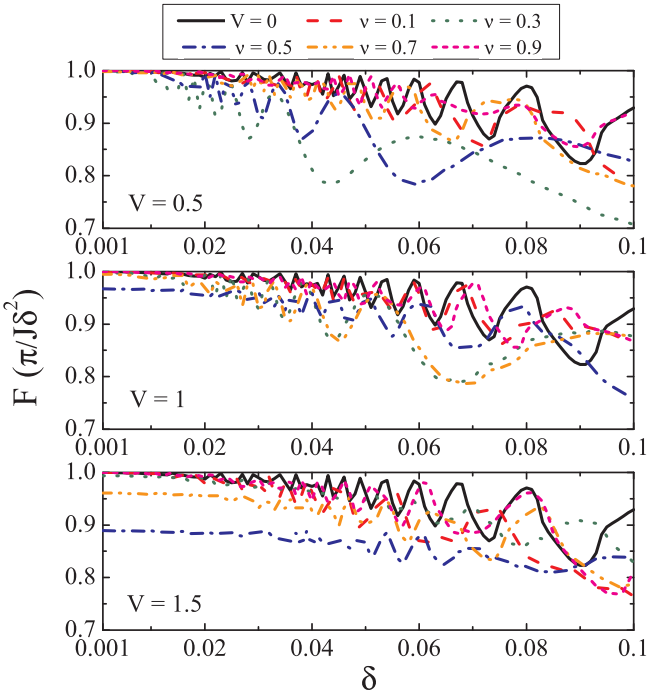

Fig. 6. Input-averaged fidelity $F(\tau)$ evaluated at $\tau = \pi/J\delta^2$ versus δ for several channel configurations including $V = 0$ (homogeneous channel). Curves are obtained via exact numerical diagonalization of the full Hamiltonian [Eq. (1)] with $g = \delta J/\sqrt{\widetilde{\Omega}}$, $\pi\alpha = 0.1$, $W = 0$, and $N = 100$. In most cases the speed-fidelity tradeoff for the channel featuring the Sarma aperiodic sequence resembles that of the homogeneous channel (solid lines), with the fidelity scaling as $F \approx 1 - O(\delta^2)$.

that there is significant residual Δ. Such instabilities can also be seen in Fig. 5(a) and (b). Of course, the fidelities inevitably decay upon increasing δ and the characteristic oscillatory pattern is due to fact that the channel modes are taking part in the dynamics as higher-order interactions among the sender, receiver, and channel are setting up (the Rabi-like, two-level approximation becomes less reliable) [24,25,30]. Better fidelity outcomes, though, can still be obtained in the vicinity of the prescribed time τ.

4. Conclusions

We studied a QST protocol through a spin channel featuring an aperiodic distribution of local magnetic fields, what is able to induce a localization-delocalization transition when the parameters are suitable. By weakly attaching two more spins to act as sender and receiver at each end of the channel we showed that it is still possible for them to communicate with great fidelity as long as their energies match with the center of the channel band, wherein extended states are available. We also found that the channel features speed-fidelity tradeoff comparable to its fully homogeneous counterpart [30]. What is more, the same protocol can be used for creating end-to-end bipartite entanglement.

In general, weak-coupling models are versatile for they are also useful in a variety of quantum information processing tasks. They can be used, for instance, for spanning decoherence-free subpaces [47]. Different models and topologies have also been addressed for the sake of generating long-distance entanglement [48,49,26] with some experiments being carried out along (see, e.g. [50]). Further extensions of this work may follow in that direction, possibly in view of state-of-the-art technology [14].

Declaration of Competing Interest

The authors declare that they have no known competing financial interests or personal relationships that could have appeared to influence the work reported in this paper.

Acknowledgments

This work was supported by CNPq, CAPES, and FINEP, CNPq-Rede Nanobioestruturas, and FAPEAL.

References

[1] J.I. Cirac, P. Zoller, H.J. Kimble, H. Mabuchi, Phys. Rev. Lett. 78 (1997) 3221.
[2] H.J. Kimble, Nature 453 (2008) 1023.
[3] S. Bose, Phys. Rev. Lett. 91 (2003) 207901.
[4] T.J.G. Apollaro, S. Lorenzo, F. Plastina, Int. J. Mod. Phys. B 27 (2013) 1345035.
[5] G.M. Nikolopoulos, I. Jex (Eds.), Quantum State Transfer and Network Engineering, Springer-Verlag, Berlin, 2014.
[6] G.M.A. Almeida, F.A.B.F. de Moura, M.L. Lyra, Phys. Lett. A 382 (2018) 1335.
[7] C.K. Burrell, J. Eisert, T.J. Osborne, Phys. Rev. A 80 (2009) 052319.
[8] J. Allcock, N. Linden, Phys. Rev. Lett. 102 (2009) 110501.
[9] F. Izrailev, A. Krokhin, N. Makarov, Phys. Rep. 512 (2012) 125–254.
[10] F.A.B.F. de Moura, M.L. Lyra, Phys. Rev. Lett. 81 (1998) 3735–3738.
[11] F.M. Izrailev, A.A. Krokhin, Phys. Rev. Lett. 82 (1999) 4062–4065.
[12] U. Kuhl, F.M. Izrailev, A.A. Krokhin, H.-J. Stöckmann, Appl. Phys. Lett. 77 (2000) 633–635.
[13] U. Kuhl, F.M. Izrailev, A.A. Krokhin, Phys. Rev. Lett. 100 (2008) 126402.
[14] H.P. Lüschen, S. Scherg, T. Kohlert, M. Schreiber, P. Bordia, X. Li, S. Das Sarma, I. Bloch, Phys. Rev. Lett. 120 (2018) 160404.
[15] G.M.A. Almeida, F.A.B.F. de Moura, T.J.G. Apollaro, M.L. Lyra, Phys. Rev. A 96 (2017) 032315.
[16] G. De Chiara, D. Rossini, S. Montangero, R. Fazio, Phys. Rev. A 72 (2005) 012323.
[17] D. Burgarth, S. Bose, New Journal of Physics 7 (2005) 135.
[18] D.I. Tsomokos, M.J. Hartmann, S.F. Huelga, M.B. Plenio, New J. Phys. 9 (2007) 79.
[19] D. Petrosyan, G.M. Nikolopoulos, P. Lambropoulos, Phys. Rev. A 81 (2010) 042307.
[20] N.Y. Yao, L. Jiang, A.V. Gorshkov, Z.-X. Gong, A. Zhai, L.-M. Duan, M.D. Lukin, Phys. Rev. Lett. 106 (2011) 040505.
[21] A. Zwick, G.A. Álvarez, J. Stolze, O. Osenda, Phys. Rev. A 84 (2011) 022311.
[22] S. Ashhab, Phys. Rev. A 92 (2015) 062305.
[23] A. Kay, Phys. Rev. A 93 (2016) 042320.
[24] A. Wójcik, T. Łuczak, P. Kurzyski, A. Grudka, T. Gdala, M. Bednarska, Phys. Rev. A 72 (2005) 034303.
[25] A. Wójcik, T. Łuczak, P. Kurzyski, A. Grudka, T. Gdala, M. Bednarska, Phys. Rev. A 75 (2007) 022330.
[26] S.M. Giampaolo, F. Illuminati, New J. Phys. 12 (2010) 025019.
[27] M.P. Estarellas, I. D'Amico, T.P. Spiller, Phys. Rev. A 95 (2017) 042335.
[28] S. Paganelli, S. Lorenzo, T.J.G. Apollaro, F. Plastina, G.L. Giorgi, Phys. Rev. A 87 (2013) 062309.
[29] G.M.A. Almeida, C.V.C. Mendes, M.L. Lyra, F.A.B.F. de Moura, Ann. Phys. 398 (2018) 180.
[30] G.M.A. Almeida, Phys. Rev. A 98 (2018) 012334.
[31] S. Das Sarma, S. He, X.C. Xie, Phys. Rev. Lett. 61 (1988) 2144–2147.
[32] S. Das Sarma, S. He, X.C. Xie, Phys. Rev. B 41 (1990) 5544–5565.
[33] R. Farchioni, G. Grosso, G.P. Parravicini, Phys. Rev. B 47 (1993) 2394.
[34] H. Cruz, S. Das Sarma, J. Physique I 3 (1993) 1515.
[35] F.A.B.F. de Moura, M.L. Lyra, F.D. Dominguez-Adame, V.A. Malyshev, Phys. Rev. B 71 (2005) 104303.
[36] L. Gong, P. Tong, Phys. Rev. B 76 (2007) 085121.
[37] L.Y. Gong, H. Zhu, S.M. Zhao, W.W. Cheng, Y.B. Sheng, Phys. Lett. A 376 (2012) 3026.
[38] L.Y. Gong, L. Wei, S.M. Zhao, W.W. Cheng, Phys. Rev. E 86 (2012) 061122.
[39] W.W. Cheng, L.Y. Gong, C.J. Shan, Y.B. Sheng, S.M. Zhao, Eur. Phys. J. D 67 (2013) 121.
[40] E. Lazo, Eur. Phys. J. D 71 (2017) 1.
[41] T. Liu, X.L. Gao, S.H. Chen, H. Guo, Phys. Lett. A 381 (2017) 3683.
[42] T. Liu, Y.-Y. Yan, H. Guo, Phys. Rev. B 96 (2017) 174207.
[43] T. Liu, H. Guo, Phys. Lett. A 382 (2018) 3287.
[44] W.K. Wootters, Phys. Rev. Lett. 80 (1998) 2245–2248.
[45] F.A.B.F. de Moura, J. Phys.: Cond. Mat. 22 (2010) 435401.
[46] F.A.B.F. de Moura, J.M. Int, Phys. C 22 (2011) 63.
[47] W. Qin, C. Wang, X. Zhang, Phys. Rev. A 91 (2015) 042303.
[48] L. Campos Venuti, S.M. Giampaolo, F. Illuminati, P. Zanardi, Phys. Rev. A 76 (2007) 052328.
[49] S.M. Giampaolo, F. Illuminati, Phys. Rev. A 80 (2009) 050301.
[50] S. Sahling, G. Remenyi, C. Paulsen, P. Monceau, V. Saligrama, C. Marin, A. Revcolevschi, L.P. Regnault, S. Raymond, J.E. Lorenzo, Nature Phys. 11 (2015) 255.